American Journal of Engineering Research (AJER)
e-ISSN: 2320-0847 p-ISSN : 2320-0936
Volume-10, Issue-04, pp: 15-35
www.ajer.org
Research Paper Open Access

Evaluation of Performance Parameters of Spark Ignition Engine Using Artificial Neural Network

ADIO, T. A. [1], ADEGBAYO O.O[1], ALAJEDE A.M[1] and OKUNLOLA G. S[1].
[1] *Department of Mechanical Engineering, The Polytechnic, Ibadan*

ABSTRACT
Spark ignition engine, SIE is a device that operates on an open thermodynamic cycle which is used to convert the chemical energy of a fuel to mechanical energy for the purpose of power generation. Emissions from this device have been found to be a major contributory factor to global warming due to incomplete combustion and these have adverse effect on human's life and properties. This study therefore evaluated the performance parameters of SIE making full use of artificial neural network, ANN.
The effects of variation in the values of three operating parameters (engine-load, engine-speed and equivalence-ratio) of SIE on the values of five performance parameters (Brake-mean-effective-pressure, BMEP, Thermal-efficiency, Hydrocarbon-emission, HC-emission, Carbon-monoxide-emission, CO-emission and Nitrogen-Oxides-emissions, NO_x-emissions) were theoretically evaluated using Zeldovich mechanism and thermodynamic models for the combustion process. A 4-stroke cylinder horizontal shaft SIE coupled to a 6.0 kVA alternator (electric generator) was selected for the study and for proper loading of the engine; a locally fabricated electric load simulator was used. Under varied conditions of operating parameters, BSFC, Brake-power, BP and Exhaust-Gas-Temperature, EGT were experimentally obtained. The results were modeled for performance parameters predictions using ANN tool implemented in MATLAB 7.9 environment. The operating parameters were considered as the independent parameters while BSFC, BP, BMEP, Thermal-efficiency, EGT, exhaust emissions (HC, CO and NO_x) were held as dependent parameters. Analysis of Variance (ANOVA) was performed on the results to establish any significant differences.
The theoretical results for maximum and minimum values of the five considered performance parameters against the values for operating parameters; engine-speed, engine-load and equivalence-ratio are; BMEP (357.0kpa, 3000rpm, 100%, 1.2) and (101.0kpa, 2000rpm, 0%, 0.8), thermal-efficiency (48.5%, 3000rpm, 0%, 0.8) and (19.5%, 2000rpm, 100%, 1.2), HC emission (901.0ppm, 4000rpm, 100%, 1.2) and (268ppm, 2000rpm, 0%, 0.8), CO emission (3207.0ppm, 4000rpm 100%, 1.2) and (1270.0ppm 2000rpm, 0%, 0.8), and NOx (293.5ppm, 3000rpm, 100%, 1.0) and (167.0ppm, 2000rpm, 0%, 1.2) respectively. The results obtained for the effects in the variation of engine-load and engine-speed values on BSFC, BP and EGT showed that the lowest BSFC value of 111.0g/kWh was obtained at engine-speed of 3000rpm and engine-load of 0%. BP value peaked at engine-speed of 3000rpm and engine-load of 100% with highest value of 5.7kW while lowest value of 4.3kW was obtained at engine-speed of 4000rpm and engine-load of 0%. The highest value of 601^0C was obtained at engine-speed of 4000rpm and engine-load of 100% while the lowest value of 381^0C was obtained at engine-speed of 2000rpm and engine-load of 0%. The effects of variation in the values of the operating parameters on performance parameters of SIE using ANN showed an improved result as ANOVA performed on its results and that of the experimental and theoretical results showed no significant difference at $p = 0.05$ confidence level.
The study has revealed the effects of variation in the values of the selected operating parameters on performance parameters of SIE using ANN. It also developed regression models which can be used to predict the SIE performances without consuming much time.

Date of Submission: 20-03-2021 Date of acceptance: 04-04-2021

I. INTRODUCTION

Increased concern about rising fuel prices, limited petroleum supplies and greenhouse-gas emissions, the call for more advanced, efficient and cleaner spark ignition engines, SIE for industrial and domestic usages is louder than ever. The number of spark ignition engines (electric generators) in Nigeria is increasing every day and the primary fuels which are used in these engines (gasoline and diesel) are derived from petroleum-based

crude oil. High energy costs and concerns about greenhouse gas emissions have been a motivation for the quest for more efficient internal combustion engines. The need for efficiency improvements and low emissions put compression ignition engine (CIE) in the spotlight due to their already higher efficiency compare to Spark Ignition Engines. There is much on-going research into internal combustion engines, including the use of low temperature combustion to reduce NOx emissions (Wai *et al.*, 2012) because reduced NOx, homogeneous charge compression ignition or premixed charge compression ignition (PCCI) combustion is considered to be a very promising operation type (Jae and Rolf, 2012). According to Zoran (2013) the spark ignition engines manufacturing industries is going through a period of rapid transformation. The impetus for innovation and development of advanced technologies is created by recognition of energy supply and climate change challenges, as well as awareness of market pressures and ever-increasing consumers' expectations. However, researchers' contributions to the field of energy management include simulation studies using predictive modeling tools, theoretical analyses, advanced experimentation and a combination of any of these. While high efficiency had been their primary focus, emissions and environmental impacts also have to be considered and be given high priority. High efficiency clean combustion strategies, such as homogeneous charge compression ignition (HCCI) and premixed charge compression ignition (PCCI), have been widely investigated in light-duty diesel engines. These advanced combustion strategies are of intense interest because they have the potential to significantly reduce engine emissions of particulate matter (PM) and nitrogen oxides (NOx). Zhiming *et al.*, (2012) noted that a typical PCCI management strategy utilizes combinations of high exhaust gas recirculation (EGR), EGR temperature control and modified fuel injection pressure and timing to create the necessary in-cylinder conditions for achieving the required burn trajectory. Some studies have also focused on the best ways to manage transitions between modes under transient conditions. Thus, integration of the engine management system in the automation structure has been achieved using standardized Maximum Transmission Unit, MTU interface modules. Exhaust gas emissions (NOx, SOx and CO_2) and unburnt Hydrocarbons, HC from spark ignition engines have been reported to be harmful to man's health and properties. Evaluating SIE performance as related to exhaust gas system putting into consideration the performance parameters becomes a necessity as this will assist in controlling engine operation, engine efficiency and performance as well as extended the scope of applications to enhance a safer and conducive environment that is free of pollutants and reduced intensity of ultraviolet rays.

II. OBJECTIVES

The aim of this study was to evaluate the performance parameters of spark ignition engine using theoretical, experimental ANN methods.

The specific objectives are:

i. To determine theoretically some selected performance parameters of SI engine
ii. To determine experimentally some selected performance parameters of SI engine
iii. To predict the performance parameters of SI engine using Artificial Neural Network (ANN)
iv. To model the results obtained through theoretical, experimental and ANN methods for speedy prediction of the selected SI engine performance parameters.

III. RESEARCH METHODOLOGY

In this work, theoretical evaluation, experimental evaluation, prediction of performance parameters using ANN and statistical evaluation of SI engine were performed. The results of the theoretical evaluation and experimental evaluation were then compared with the corresponding results from ANN prediction to validate the accuracy of the results. In this work, theoretical analysis, experimental analysis, simulation using ANN and statistical analysis of SI engine were performed. For the purpose of theoretical analysis of SI operation, a two-zone quasi-dimensional cycle model was used. The results of the model were compared with experimental data to demonstrate the validity of the model.

The engine performance parameters that were theoretically analyzed include;

Engine emissions

The formation of various oxides of Nitrogen (NO_x) is complex and depends on a series of reactions such as the Zeldovich mechanism:

$$O + N_2 \longrightarrow NO + N \quad (3.1)$$

$$N + O_2 \longrightarrow NO + O \quad (3.2)$$

$$N + OH \longrightarrow NO + H \quad (3.3)$$

And NO_2 is formed from NO from the reaction below:

$$NO + HO_2 \longrightarrow NO_2 + OH \quad (3.4)$$

$$NO_2 + O \longrightarrow NO + O_2 \quad (3.5)$$

The rate of formation of NO via reactions above is given by:

$$\frac{d[NO]}{dt} = K_1^+ [O][N_2] + K_2^+ [N][O_2]^+$$
$$K_3^+ [N][OH] - K_1^- [NO][N] - K_2 [NO][O] - K_2^- [NO][H] - K_3^- [NO][H] \quad (3.6)$$

Equation 3.6 was used to predict the emission of NOx

CO formation is one of the principal reaction steps in the hydrocarbon combustion mechanism, which may be summarized by:

$$RH \longrightarrow R \longrightarrow RO_2 \longrightarrow RCHO \longrightarrow RCO \longrightarrow CO \quad (3.7)$$

Where R stands for the hydrocarbon radical

$$CO + OH \longrightarrow CO_2 + H \quad (3.8)$$

$$K_{co}^+ = 6.76 \times 10^{10} \exp\left[\frac{T}{1102}\right] cm^3/gmol \quad (3.9)$$

Equation 3.7 was used to predict the emission of CO

The level of unburned hydrocarbons can be predicted using the rate expression below.

$$\frac{d(HC)}{dt} = -6.7 \times 10^{15} \exp\left[\frac{-18,735}{T}\right] \overline{X}_{HC}\, \overline{X}_{o2} \left(\frac{P}{RT}\right)^2 \quad (3.10)$$

Where d (HC) denotes concentration in moles per cubic centimeter, $\overline{X}_{HC}$ and $\overline{X}_{02}$ is the mole fraction of HC and O_2 respectively, t is time in seconds, T is temperature in Kelvin and the density term (P/RT) has units of mole per cubic centimeter. **Equation 3.10 was used to predict the emission of HC**

Mean effective pressure

The cylinder pressure (ΔP) after the start of combustion changes due to the pressure rise, due to combustion (ΔP_c) and a pressure change due to the volume change (ΔP_v).

$$\Delta P = \Delta P_c + \Delta P_v \quad (3.11)$$

As the crank angle (θ) increases to its next value (θ_{i+1}), the volume changes from V_i *to* V_{i+1}, and the pressure changes from P_i *to* P_{i+1}. The pressure changes can be modeled by a polytrophic process with an exponent K. substituting for ΔP_v in eq. 3.11

$$P_{i+1} - P_i = \Delta P_c + P_i \left[\left(\frac{V_i}{V_{i+1}}\right)^K - 1\right] \quad (3.12)$$

From which ΔP_c can be evaluated:

$$\Delta P_c = P_{i+1} - P_i \left[\left(\frac{V_i}{V_{i+1}}\right)^K\right] \quad (3.13)$$

The pressure rise has to be referenced to a datum volume for example the clearance volume (V_c) at tdc because ΔPc is not directly proportional to mass fraction burned since combustion process is not occurring at constant volume.

$$\Delta P_c^* = \Delta Pc\, V_i / V_c \quad (3.14)$$

Where ΔP_c^* is the pressure rise due to combustion referenced to datum at V_c

The end of combustion occurs after N increment when the pressure rise due to combustion becomes zero. The reference pressure rise due to combustion is proportional to the mass fraction burned (mfb) then,

$$(mfb) = \sum_0^1 \Delta P_c^* / \sum_0^N \Delta P_c^* \quad (3.15)$$

Combustion process modeling

The combustion chamber is divided into two zones which are the burned zone and the unburned zone. The two zones are separated by a flame front.

The mass burning rate was modeled by equation 3.16:

$$\frac{dM_b}{dt} = A_{fl} \cdot e^{ST} \qquad 3.16$$

The turbulent flame front speed (ST) was modeled by equation 3.17:

$$ST = SL.f \cdot \frac{\left({}^{e_u}/_{e_b}\right)}{\left[\left({}^{e_u}/_{e_b}\right) - 1\right] \times M_b + 1} \qquad 3.17$$

Where f is a turbulent flame factor defined by equation 3.18:

$$f = 1.0.0018 \times rpm \qquad 3.18$$

The heat interaction between the burned and unburned zones in the combustion chamber was modeled by equation 3.19:

$$\frac{-dQ_{ht}}{dt} = A\left[0.26\frac{k}{B}\left(\frac{V_p.B}{\mu}\right)^{0.7}(T - T_w) + 0.69\sigma(T_-^4 T_w^4)\right] \qquad 3.19$$

The gas pressure and temperature during the compression stage are calculated using equation 3.20 and 3.21

$$\frac{dp}{d\theta} = \left[-\left(1 + \frac{R}{C_V}\right) \cdot P.\frac{dv}{d\theta} - \frac{R}{C_V} \cdot \frac{dQ_{cr}}{d\theta} + \frac{R}{C_V} \cdot \frac{dQ_{ht}}{d\theta}\right] \qquad 3.20$$

$$\frac{dT}{d\theta} = T \cdot \left(\frac{1}{p} \cdot \frac{dp}{d\theta} + \frac{1}{V} \cdot \frac{dV}{d\theta}\right) \qquad 3.21$$

The cylinder pressure and the temperature of burned and unburned zones was modeled using equations 3.22, 3.23 and 3.24

$$\frac{dT_u}{d\theta} = \frac{1}{N_u.C_{p,u}} \cdot \frac{dQ_{ht,u}}{d\theta} + \frac{V_u}{N_u.C_{p,u}} \cdot \frac{dp}{d\theta} - \frac{1}{N_u.C_{p,u}} \cdot \frac{dQ_{cr,u}}{d\theta} \qquad 3.22$$

$$\frac{dT_b}{d\theta} = \frac{P}{N_b.R} \cdot \left[\frac{dV}{d\theta} - \left(\frac{R.T_b}{P} - \frac{R.T_u}{P} \cdot \frac{MW_b}{MW_u}\right) \cdot \frac{dN_b}{d\theta} - \frac{V_u.R}{P.C_{p,u}} \cdot \frac{dP}{d\theta} - \frac{R}{P.C_{p,u}} \cdot \frac{dQ_{ht,u}}{d\theta} + \frac{R}{P.C_{p,u}} \cdot \frac{dQ_{cr,u}}{d\theta} + \frac{V}{P} \cdot \frac{dP}{d\theta}\right] \qquad 3.23$$

$$\frac{dP}{d\theta} = \left[\frac{\left[p\frac{dV}{d\theta} \cdot \left(1 + \frac{C_{v,b}}{R}\right) + \left(\frac{C_{v,u}}{C_{p,u}} - \frac{C_{v,b}}{C_{p,u}}\right) \cdot \frac{dQ_{ht,u}}{d\theta} + \left(e_b - e_u \cdot \frac{MW_b}{MW_u}\right) \cdot \frac{dN_b}{d\theta}\right]}{\left[\frac{C_{v,u}}{C_{p,u}} \cdot V_u - \frac{C_{v,b}}{C_{p,u}} \cdot V_u + \frac{C_{v,b}}{R} \cdot V\right]}\right.$$

$$\left. - \frac{\left(C_{v,b} \cdot \left(T_b - T_u \cdot \frac{MW_b}{MW_u}\right)\right)\frac{dN_b}{d\theta} + \left(\frac{C_{v,u}}{C_{p,u}} - \frac{C_{v,b}}{C_{p,u}}\right) \cdot \frac{dQ_{cr,u}}{d\theta} + \frac{dQ_{cr}}{d\theta} - \frac{dQ_{ht}}{d\theta}}{\left[\frac{C_{v,u}}{C_{p,u}} \cdot V_u - \frac{C_{v,b}}{C_{p,u}} \cdot V_u + \frac{C_{v,b}}{R} \cdot V\right]}\right] \qquad 3.24$$

(Suvendu and Om Prakash, 2013)

A computer program was written to solve the thermodynamic models. Equations 3.20 to 3.24 were solved by the Runge-Kutta method using MATLAB software.

Experimental Analysis

A 4-stroke cylinder horizontal shaft spark ignition engine coupled to a 6.0kVA alternator (electric generator) was used to conduct the experiments. The engine was run on 100% petrol fuel. Some modifications were made on the SI engine's fuel supply line to allow fuel consumption (FC) and engine speed to be measured. Table1 shows the engine's specification for the engine that was used.

Materials and apparatus

The following materials and apparatus were used for the experiment in this research;
Elepaq 6.0kVA electric generator
Hydra PT-110 Non-contact laser Tachometer
Locally fabricated electric load simulator
Burette
Retort stand
Fuel tank
Hose
Petrol fuel
Fuel tank stand
Stop watch
Thermocouple
Torque meter

Engine load

A locally fabricated electric load simulator was used in this section. This load simulator consist of twenty nine different light bulbs of 200 W each and two light bulb of 100 W (total of 6.0kW) wired in parallel, with every two bulbs sharing a switch, to allow easy loading and flexible testing. A schematic diagram of the load simulator is illustrated in Figure 1

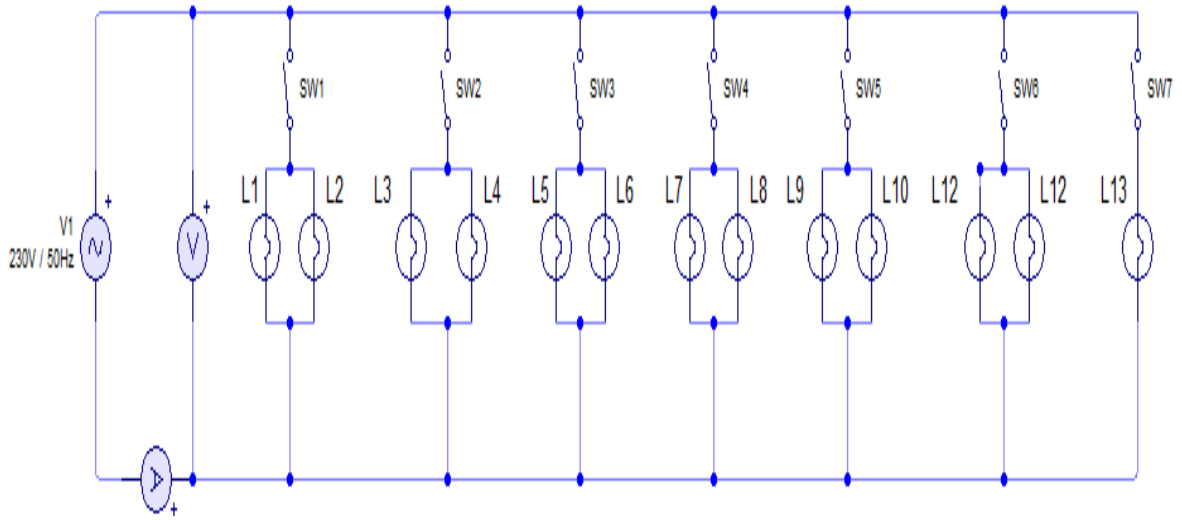

Figure 1: Circuit Diagram of the Load Simulator

Table 1: Engine Specifications

S/N	Parameters	Value
	Maker	Elepaq
	Type	Air cooled, SI engine
	Number of cylinder	1
	Bore –Stroke (mm)	60 x 42 mm
	Connecting rod	78 mm
	Displacement	118 cm^3
	Clearance volume	10.05 cm^3
	Cycle	Four stroke
	Maximum speed	5500 rpm
	Maximum torque	7.4 Nm
	Maximum power	7.0 kW
	Dimension	305 x 341 x 318 mm
	Dry weight	13 kg

SW: switch
L: load
V: voltmeter
A: Ammeter

Engine speed
Five different engine speeds were considered (2000, 2500, 3000, 3500 and 4000) in this section. The actual speed in rpm was measured by using a hand hold PT-110 Non-Contact Laser Tachometer.

Specific fuel consumption
The fuel consumption was measured by using a calibrated burette and a stop watch. The amount of fuel consumed for every two minutes was obtained and recorded. i.e.,

$$xml/2minutes = \frac{x}{120}\ ml/s \qquad 3.25$$

Experimental procedures
The experiment set up that was used is shown in Figure 2. Before each set of data was taken, the engine was allowed to run for about 20 minutes to warm up. Procedures for collecting each data point are as follows:
The engine speed was set at 2000rpm using tachometer to get the actual speed at zero (0%) loading condition (0watts). Then, fuel consumption per every 2 minutes, engine torque, exhaust gas temperature, ammeter reading and voltmeter reading were measured and recorded. Engine load was then increased from 0watts (0%) to 6.0kW (100%) in steps of 1.5kW (25%) and the above measurements were repeated. Engine speed was then increased from 2000rpm to 4000rpm in steps of 500rpm and the above procedures were repeated.

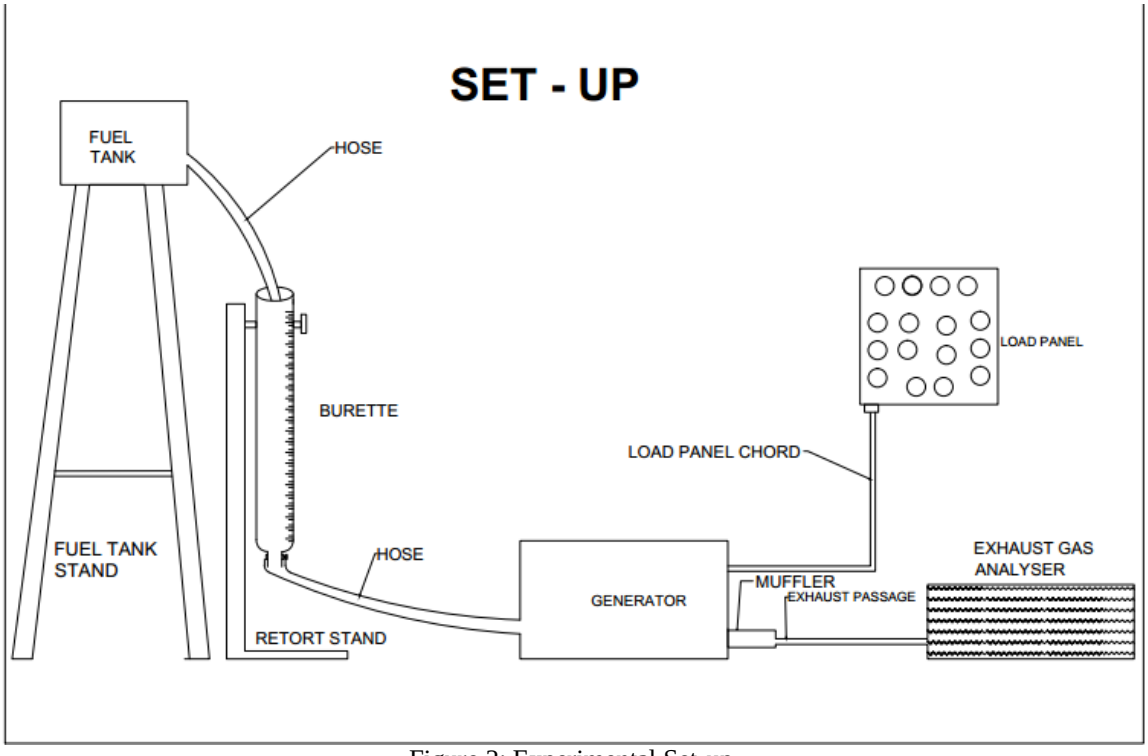

Figure 2: Experimental Set-up

Prediction of performance parameters using ANN
Investigation was made on the effect of varying three operating parameters on the performance characteristics of spark ignition engines using different artificial neural networks. The operating parameters that were varied are termed as input parameters while performance parameters are termed as output parameters.

Input parameters
The input parameters that were considered are:
(i) Engine load
(ii) Engine speed
(iii) Equivalence ratio

Output parameters

The output parameters are made up of eight performance parameters. The parameters that were considered are:

(i) Brake Specific fuel consumption (BSFC)
(ii) Brake power (BP)
(iii) Brake mean effective pressure (BMEP)
(iv) Thermal efficiency (η_{th})
(v) Exhaust gas temperature (EGT)
(vi) Unburned Hydrocarbon (HC)
(vii) Carbon monoxide (CO)
(viii) Oxides of Nitrogen (NO_X)

The ANN model is

$$y_k = \sum_{l=1}^{N_H} W_i \, \varphi \left(\sum_{j=1}^{N} W_{ij} \, I_j \right) \qquad 3.26$$

Where

y_k = outputs of the ANN model
K = number of output
N_H = number of neurons in the hidden layers
H = number of hidden layers
W_i = synaptic weights connecting the hidden layers with output
W_{ij} = synaptic weights connecting the inputs to the hidden layers
N = number of inputs
φ = activation / transfer function
I_j = Inputs to the ANN model

ANN prediction procedure

All the engine data patterns available from theoretical and experimental results were partitioned randomly into three sets. 70% of the data was used for training the network, 15% of the data will be used for validating the network and the remaining 15% of the data was used to test the network. Network training can be made more efficient if certain preprocessing steps such as normalization are performed on the network inputs and target outputs. Normalization step was applied to both the input vectors and the target vectors in the data set. The network output was then reversed transformed back into the units of the original target data. Equation 3.26 shows the ANN model used in this work

Several ANN parameters were investigated in details in order to get efficient network architecture for the ANN model. The ANN parameters that were considered are:

Activation / transfer function: Three different activation functions (Purelin, Logsig and Tansig) which are the most commonly used and most accurate activation functions available from literatures were investigated and log sig was picked and used.

Number of hidden layers: One, two and three hidden layers were considered at several levels and at different combinations using literature as guide.

Training function: Three different training functions trainlm (Levenberg – Marquardt algorithm), trainrp (Resilient back propagation algorithm) and trainscg (Scaled conjugate gradient) were investigated using literatures as guide and trainlm was picked and used in this work.

Number of neurons in the hidden layers: Several iterations at several levels using different combinations of neurons were investigated in details after which 12 neurons, 8 neurons and 5 neurons in the first, second and third hidden layers respectively gave the best result and was therefore used in this work.

Statistical Analysis

All statistical tests shared the same principle which means that they compare the observed or predicted results with an expected or actual value based on dataset used and come up with a so – called test statistic.

In this work, there were three sets of results, which are the theoretical, experimental and the ANN predicted results. The best and most popular statistical methods for analyzing differences between two groups of data sets is t-test and was therefore used in this work to test variance between (1) theoretical and ANN predicted result and (2) experimental and ANN results.

The t-test gives an indication of the separateness of two sets of measurement and to check whether two sets of data are essentially different. The typical way of doing these is with the null hypothesis that means of the two sets of data are equal. The equation of t-test is given below:

$$t = \frac{\overline{X_1} - \overline{X_2}}{\frac{\overline{var1}}{n} + \frac{\overline{var2}}{n}} \qquad 3.27$$

Where
X_1 = experimental or theoretical values
X_2 = ANN predicted values
$\overline{X_1}$ = mean of X_1
$\overline{X_2}$ = mean of X_2
Var_1= Variance = standard deviation squared (SD^2) of X_1
Var_2= Variance = standard deviation squared (SD^2) of X_2
n = number of samples
t = t stat (calculated value of t)
Degree of freedom = $(n_1 + n_2) - 2$
The null hypothesis is $\mu_1 - \mu_2 = 0$
This indicate that there is no significant difference between the two means
The confidence level that was used is 95% = 0.05 level of significance
The criterion is: Reject the null hypothesis if
t stat > t critical
Where, t critical = t tabulated
Regression equations and R^2 values were also generated for the results using historical data design tool of Design Expert 6.0.8. However, the data involved in this study were too voluminous to be analysed manually, this made it necessary to employ the use of statistical software packages developed (SPSS 17.0) to assist in the analyses of t-test to enhance speed and accuracy.

IV. RESULTS AND DISCUSSIONS

Theoretical Evaluation

The effects of variation in the values of three operating parameters of SI engine on the values of five performance parameters were evaluated in this section. Table 1 shows the theoretical results obtained in this work. It can be seen from this table that BMEP peaked at engine speed of 3000rpm, engine load of 100% and equivalence ratio of 1.2. The maximum BMEP value of 357.0kPa was obtained at engine speed of 3000rpm, engine load of 100% and equivalence ratio of 1.2 while the lowest value of 101.6kpa was obtained at engine speed of 2000rpm, engine load of 0% and equivalence ratio of 0.8. Thermal efficiency reduces with increase in both engine load and equivalence ratio but peaked at engine speed of 3000rpm. The highest thermal efficiency of 48.5% was achieved at engine speed of 3000rpm while the lowest value of 19.5% was achieved at engine load of 100%, equivalence ratio of 1.2 and engine speed of 2000rpm.

It can also be seen from this table that both HC and CO emissions increase with increase in engine load, engine speed and equivalence ratio, i.e., a direct proportional relationship. The highest HC emission of 901.0ppm was obtained at engine load of 100%, engine speed of 4000rpm and equivalence ratio of 1.2 while the lowest emission of 268ppm was obtained at engine load of 0%, engine speed of 2000rpm and equivalence ratio of 0.8. Similarly, the highest CO emission of 3207.0ppm was obtained at engine load of 100%, engine speed of 4000rpm and equivalence ratio of 1.2 while the lowest emission of 1270.0ppm was obtained at engine load of 0%, engine speed of 2000rpm and equivalence ratio of 0.8. This table also shows that NOx emission peaked at engine speed of 3000rpm engine load of 100% and equivalence ratio of 1.0. The lowest NOx emission of 167.0ppm

Table 1 Theoretical Results

S/N	Load (%)	Speed (rpm)	Equivalence Ratio	BMEP (kPa)	Thermal Efficiency (%)	HC Emission (PPM)	CO Emission (PPM)	NO_x Emission (PPM)
1.	0	2000	0.8	101.6	39.5	268.0	1270.0	175.0
2.	0	3000	0.8	161.5	48.5	334.5	1402.0	202.5
3.	0	4000	0.8	108.0	42.5	403.5	1535.5	185.0
4.	50	2000	0.8	165.0	35.0	368.5	1436.0	207.5
5.	50	3000	0.8	215.0	45.5	435.0	1568.5	233.5
6.	50	4000	0.8	165.4	38.0	501.0	1702.5	217.0
7.	100	2000	0.8	207.5	32.0	467.5	1602.5	240.5
8.	100	3000	0.8	268.0	42.0	535.0	1736.0	267.0
9.	100	4000	0.8	224.0	36.1	601.5	1867.5	251.0
10.	0	2000	1.0	131.0	33.5	402.0	1935.0	184.0
11.	0	3000	1.0	191.0	44.0	467.0	2068.0	226.0
12.	0	4000	1.0	137.5	37.5	535.0	2203.0	193.5
13.	50	2000	1.0	194.5	30.5	501.0	2103.0	217.5
14.	50	3000	1.0	244.0	40.2	567.5	2234.5	261.0
15.	50	4000	1.0	193.5	35.0	634.0	2368.0	227.0
16.	100	2000	1.0	247.5	27.5	601.5	2270.0	251.0

17.	100	3000	1.0	297.0	38.0	667.0	2402.0	293.5
18.	100	4000	1.0	254.0	32.5	734.5	2536.5	260.5
19.	0	2000	1.2	191.5	25.0	567.4	2605.0	167.0
20.	0	3000	1.2	251.0	35.0	635.0	2735.5	194.5
21.	0	4000	1.2	198.5	29.0	701.5	2866.8	176.9
22.	50	2000	1.2	253.0	22.0	667.5	2768.0	201.5
23.	50	3000	1.2	305.0	32.0	734.0	2905.5	228.5
24.	50	4000	1.2	254.0	26.1	803.0	3037.7	201.0
25.	100	2000	1.2	307.0	19.5	768.5	2938.5	235.0
26.	100	3000	1.2	357.0	29.1	835.0	3070.5	261.0
27.	100	4000	1.2	314.5	27.0	901.0	3207.0	243.5

was obtained at engine load of 0%, engine speed of 2000rpm and equivalence ratio of 1.2 while the highest emission of 293.5rpm was obtained at engine load of 100%, engine speed of 3000rpm and equivalence ratio of 1.0.

The results obtained in this section may be due to the fact that the mean effective pressure peaks slightly rich of stoichiometric (between equivalence ratio of 1.0 and 1.2). For lean mixtures, the theoretical fuel conversion efficiency increases linearly as equivalence ratio decreases below 1.0 and products of combustion will be at lower temperature. Thermal efficiency increases as equivalence ratio decreases provided the mixture is not too lean. For equivalence ratio is greater than 1.0 (rich mixtures), complete combustion becomes difficult therefore CO and HC emissions tend to increase because they are products of incomplete combustion.

Experimental Evaluation

The effects in the variation in the values of engine load and engine speed on brake specific fuel consumption, BSFC, Brake power, BP and exhaust gas temperature, EGT were presented in Table 4.2 and evaluated in this section. It can be seen from Table 4.2 that BSFC has minimum value at engine speed of 3000rpm and this value increase with increase in engine load. Lowest BSFC value of 111.0g/kWh was obtained at engine speed of 3000rpm and engine load of 0%. This result may be due to fact engine friction increases rapidly above engine speed of 3000rpm leading to increase in BSFC. A similar trend is required for BP with maximum value obtained at 3000rpm. It can also be seen from this table that BP value peaked at engine speed of 3000rpm and engine load of 100% with highest value of 5.7kW while lowest value of 4.3kW was obtained at engine speed of 4000rpm and engine load of 0%. **This result may be because as engine load increased, the relative importance of engine friction decreased leading to maximum BP at engine**

Table 2:Experimental result

S/N	Load (%)	Speed (rpm)	BSFC (g/kWh)	BP (kW)	EQT (^{0}C)
1.	0	2000	118.5	4.5	381
2.	0	2500	116.5	4.7	427
3.	0	3000	111.0	4.9	433
4.	0	3500	116.0	4.7	457
5.	0	4000	121.0	4.3	482
6.	25	2000	132.0	4.5	411
7.	25	2500	124.0	4.9	437
8.	25	3000	118.0	5.1	461
9.	25	3500	123.0	4.9	486
10.	25	4000	128.0	4.5	511
11.	50	2000	139.5	4.7	441
12.	50	2500	131.5	5.1	466
13.	50	3000	125.5	5.5	441
14.	50	3500	130.5	5.2	517
15.	50	4000	135.5	4.7	541
16.	75	2000	147.5	4.9	471
17.	75	2500	139.0	5.3	496
18.	75	3000	133.0	5.5	421
19.	75	3500	138.0	5.3	546
20.	75	4000	143.0	4.9	571

21.	100	2000	155.5	5.1	501
22.	100	2500	146.5	5.5	526
23.	100	3000	140.5	5.7	551
24.	100	3500	145.5	5.5	576
25.	100	4000	150.0	5.1	601

load of 100%. This table also shows that exhaust gas temperature increases as both engine speed and engine load increase. The highest value of 601^0C was obtained at engine speed of 4000rpm and engine load of 100% while the lowest value of 381^0C was obtained at engine speed of 2000rpm and engine load of 0%. **This result may be because engine friction increase with increase in engine speed leading to maximum temperature at highest speed.**

ANN Evaluation

The effects of variation in the values of three operating parameters on eight performance parameters of SI engine were presented and discussed in this section. The operating parameters of concern are engine speed, engine load and equivalence ratio while the performance parameters considered are BSFC, BP, BMEP, Thermal efficiency, EGT, HC emission, CO emission and NO_x emission. Figure 4.1 shows the effects of engine speed and equivalence ratio on BSFC. This Figure shows that engine speed of 3000rpm gives the lowest value for BSFC and the value increases before and after this speed for all the equivalence ratios considered. From this figure, it can also be seen that BSFC increases as equivalence ratio increases from 0.8 to 1.2. The lowest value of BSFC of 125g/kWh was achieved at equivalence ratio of 0.8 and engine speed of 3000rpm while the highest value of 165g/kWh was achieved at engine speed of 2000rpm and equivalence ratio of 1.2. Figure 2 shows the effects of engine load and equivalence ratio on BSFC. From this figure it can be seen that there exist a direct proportional relationship between BSFC and engine load, i.e., BSFC values increase as engine load increases from 0% to 100% for all the equivalence ratios considered. The lowest BSFC value of 105g/kWh was obtained at engine load of 0% and equivalence ratio of 0.8 **while the highest value of 160g/kWh was obtained at engine load of 100% and equivalence ratio of 1.2.** The results obtained

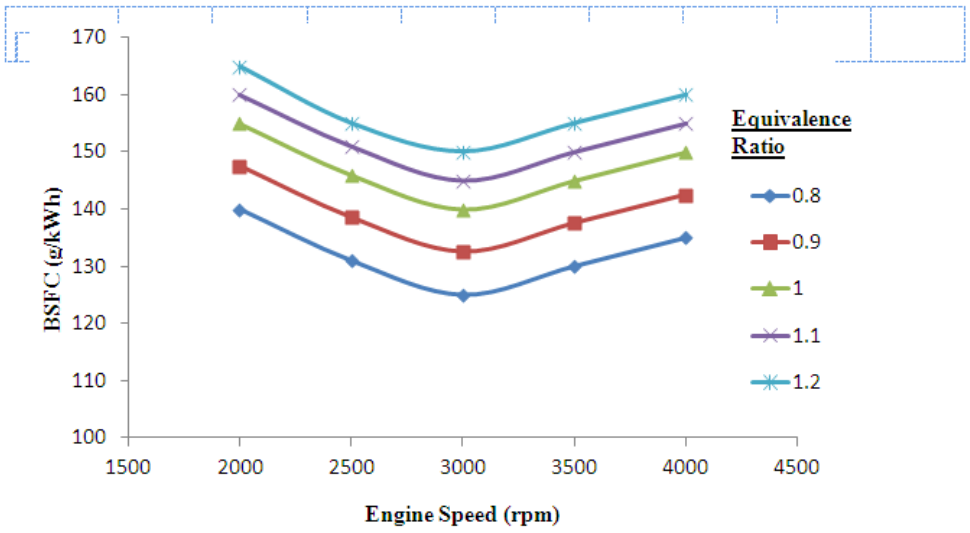

Figure 1: Effect of Engine Speed and Equivalence Ratio on BSFC

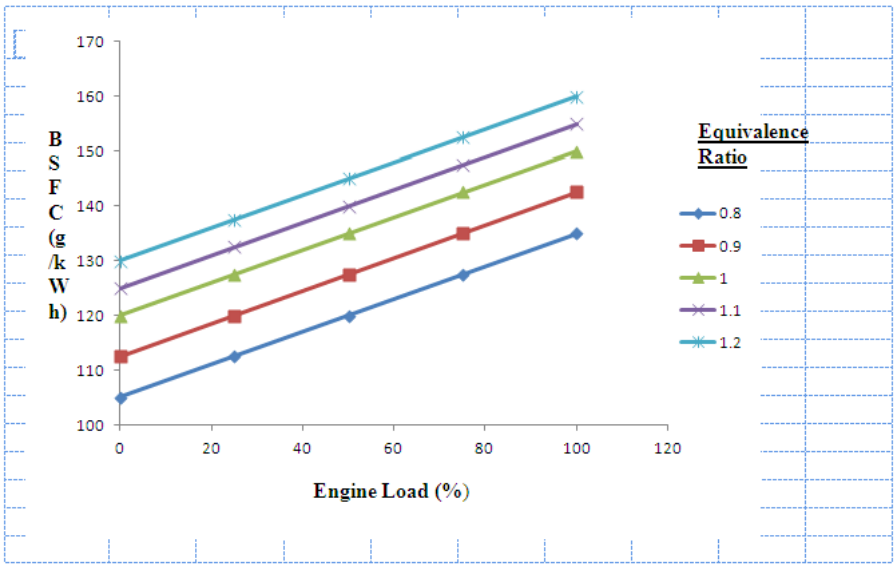

Figure 2: Effect of Engine Load and Equivalence Ratio on BSFC

Figure 4.2 may be due to the fact that as engine speed increase, both engine efficiency and engine friction predominates at higher speeds above 3000rpm. Hence, highest net engine efficiency is obtained at engine speed of 3000rpm. **This trend is repeated for BP, BMEP, thermal efficiency and NO_x emission.** Figure 3, shows that engine speed of 2000rpm gives the lowest value for BP. The value obtained increase to maximum at 3000rpm and decreases from 3000rpm to 4000rpm for different equivalence ratio considered. It can be seen from this figure that the BP increases as the equivalence ratio increased from 0.8 to 1.2. The highest value of BP of 6.6kW was obtained at engine speed of 3000rpm and equivalence ratio of 1.2 while the lowest value of 3.8kW was obtained at engine speed of 2000rpm and equivalence ratio of 0.8. Figure 4 shows the effect of engine load on BP at different equivalence ratio. From this figure, it can be seen that BP increase with increase in both engine speed and equivalence ratio. The lowest BP value of 3.0kW was obtained at engine load of 0% and equivalence ratio of 0.8 and highest BP value of 6.0kW was obtained at equivalence ratio of 1.2 and engine load of 100%. The results obtained may be because increase in engine load leads to increase in engine efficiency due to better combustion which means that highest engine load leads to better combustion. Also, increasing engine load reduces the relative importance of engine friction and heat transfer. This same trend is repeated for most of the performance parameters considered in this study. Figure 5 shows that the values obtained for BMEP values peaked at engine speed of 3000rpm for all the equivalence ratios considered. Also BMEP values increase as equivalence ratio increased from 0.8 to 1.2 for different engine speeds considered. The highest BMEP value of 356.7kPa was obtained at equivalence ratio of 1.2 and engine speed of 3000rpm while the lowest value of 216.7kPa was obtained at equivalence ratio of 0.8 and engine speed of 2000rpm. Figure 6 shows that increase in engine load leads to increase in BMEP for the entire equivalence ratio considered. Highest

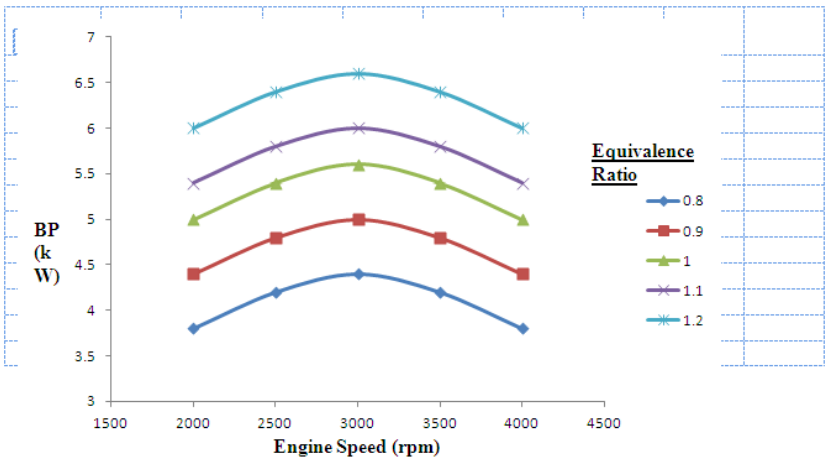

Figure 3: Effect of Engine Speed and Equivalence Ratio on BP

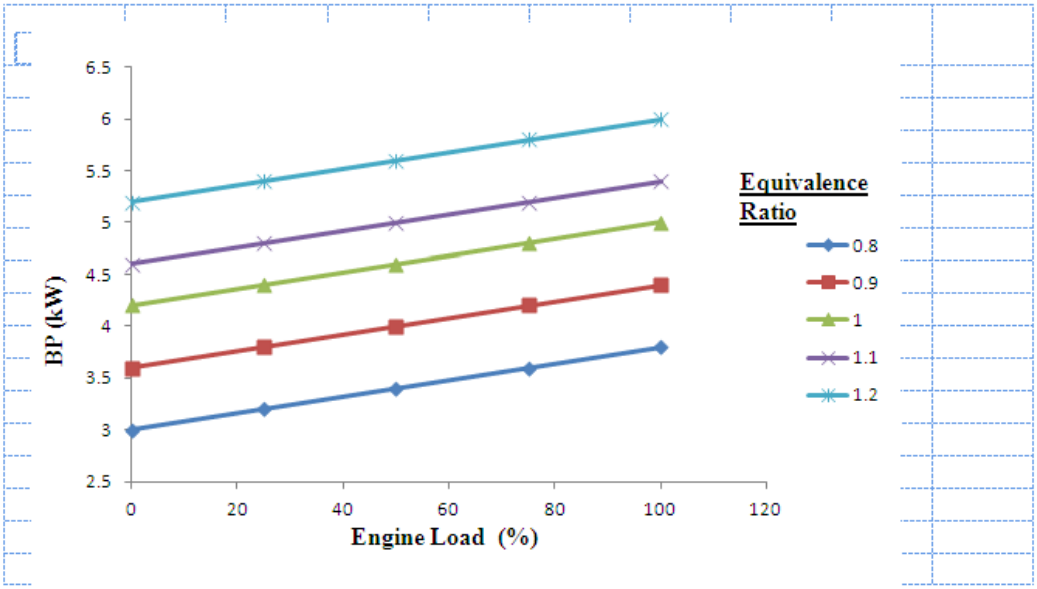

Figure 4: Effect of Engine Load and Equivalence Ratio on BP

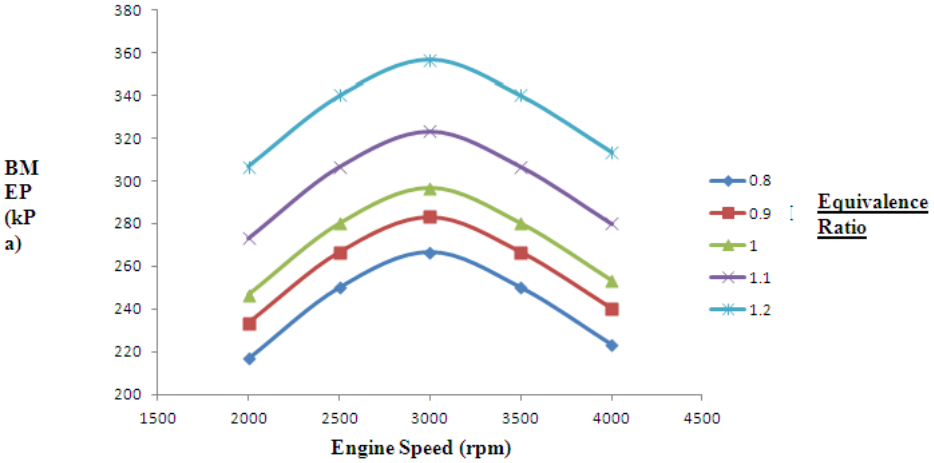

Figure 5: Effect of Engine Speed and Equivalence Ratio on BMEP

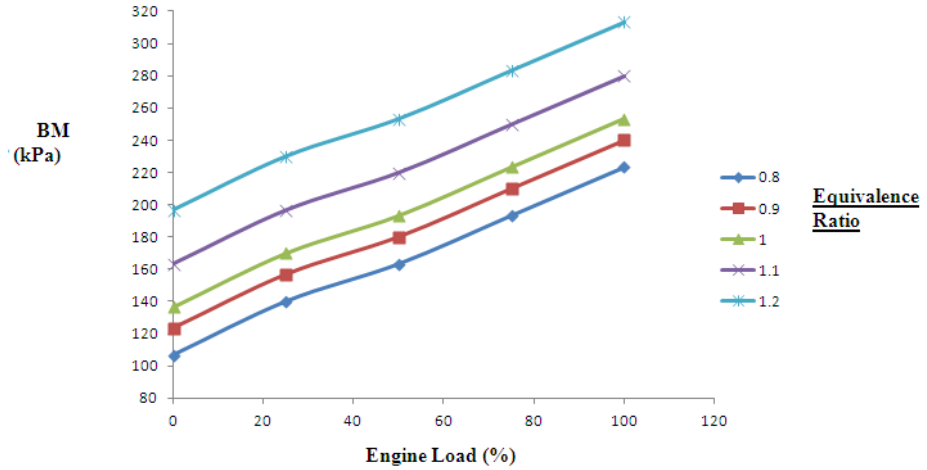

Figure 6: Effect of Engine Load and Equivalence Ratio on BMEP

BMEP value of 313.3kPa was obtained at engine load of 100% and equivalence ratio of 1.2 while the lowest value of 166.7 kPa was obtained at engine load of 0% and equivalence ratio of 0.8. Figure 4.7 shows the effects of engine speed and equivalence ratio on thermal efficiency. It can be seen from this figure that thermal efficiency reduces as equivalence ratio increases from 0.8 to 1.2 and that the values of thermal efficiency peaked at engine speed of 3000rpm for all the equivalence ratios considered. The highest value of 42% was obtained at equivalence ratio of 0.8 and engine speed of 3000rpm while the lowest value of 18% was obtained at engine speed of 2000rpm and equivalence ratio of 1.2. The highest percentage increase of 33% in thermal efficiency was obtained when equivalence ratio reduces from 1.2 to 1.1. Figure 8 shows that thermal efficiency reduces with increase in engine load for all the equivalence ratio considered. The highest value of 42% was obtained at engine load of 0% and equivalence ratio of 0.8 while the lowest value of 22.5% was obtained at engine load of 100% and equivalence ratio of 1.2. This indicates at the instance that there exist an inversely proportional relationship between thermal efficiency and engine load for all the considered equivalence ratios. Figure 4.9 shows the effects of engine speed and equivalence ratio on exhaust gas temperature, EGT. It can be seen from this figure that EGT increase in both engine speed and equivalence ratio. The highest temperature of 720^0C was obtained at engine speed of 4000rpm and equivalence ratio of 1.2 while the lowest temperature of 400^0C was obtained at engine speed of 2000rpm and equivalence ratio of 0.8. This result may be due to the fact that as engine speed increases, engine friction also increased leading to higher temperature at higher speeds. Figure 10 shows the effect of engine load and equivalence ratio on EGT. It can be seen from this figure that EGT increases with increase in both engine load and equivalence ratio. The highest temperature of 720^0C was obtained at engine load of 100% and equivalence ratio of 1.2 while the lowest temperature of 380^0C was obtained at engine load of 0% and equivalence ratio of 0.8. Figure 11 shows the result for the effects of engine speed HC emission at different equivalence ratios.

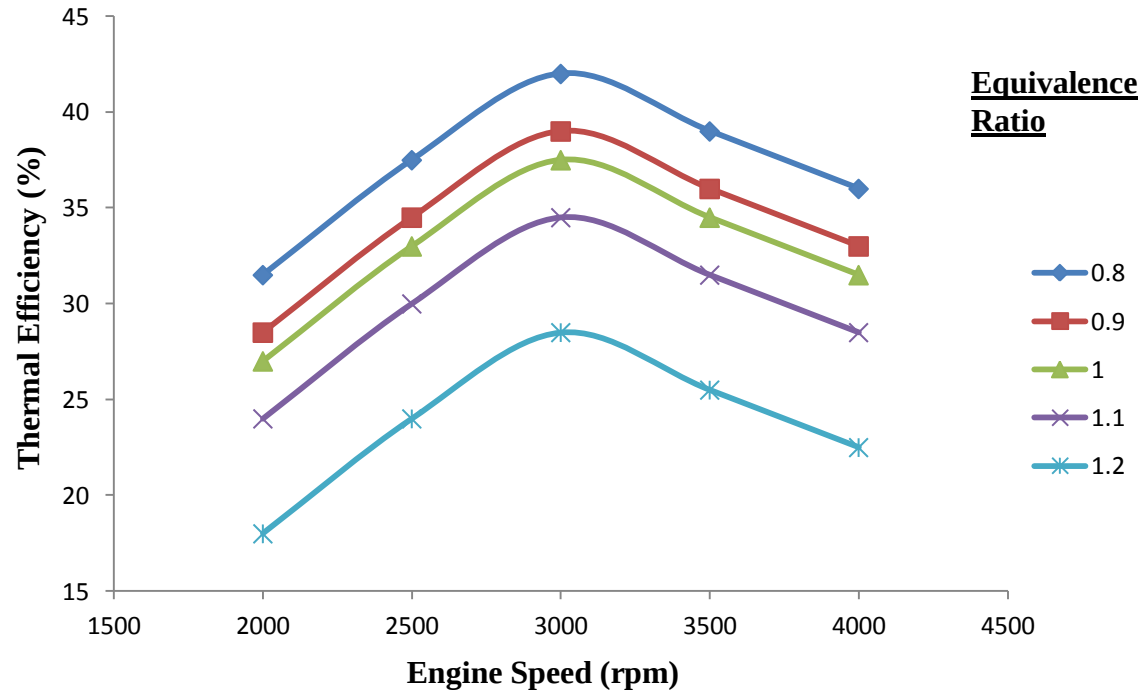

Figure 7: Effect of Engine Speed and Equivalence Ratio on Thermal Efficiency

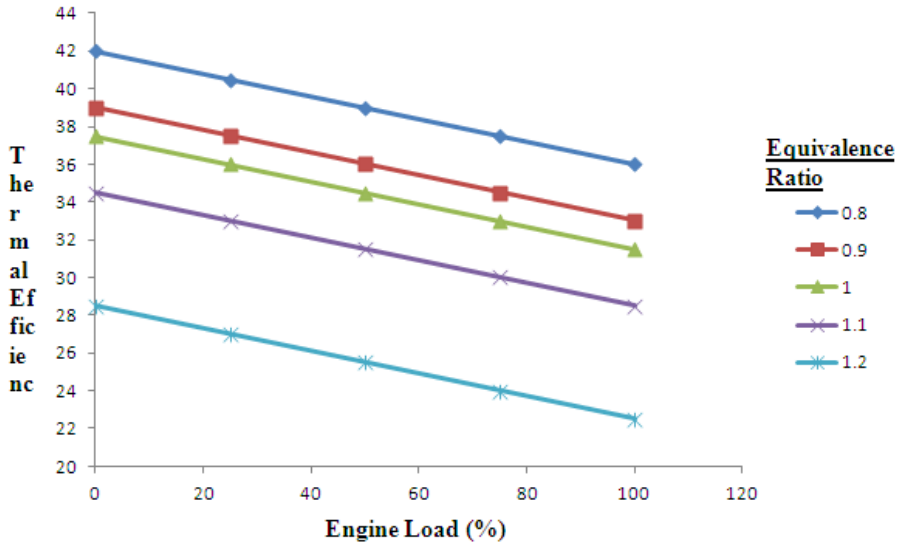

Figure 8: Effect of Engine Load and Equivalence Ratio on Thermal Efficiency

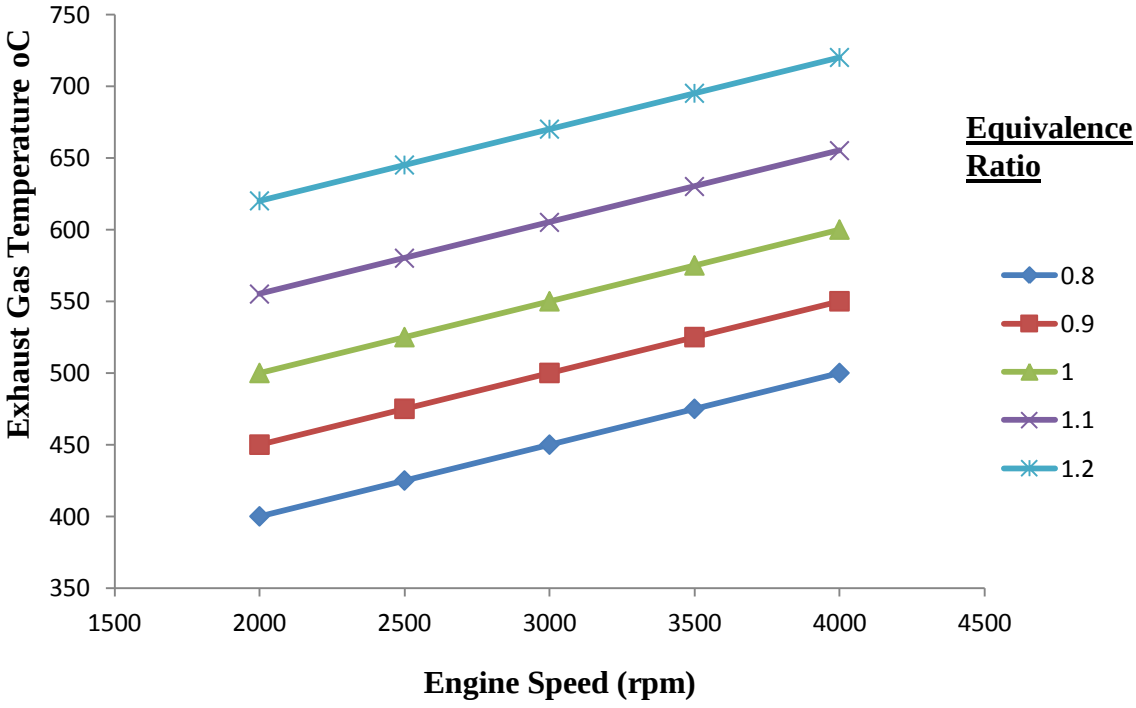

Figure 9: Effect of Engine Speed and Equivalence Ratio on Exhaust Gas Temperature

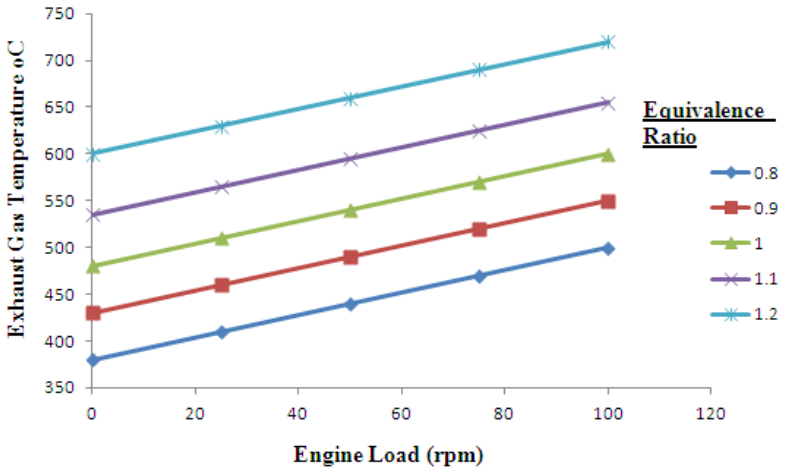

Figure 10: Effect of Engine Load and Equivalence Ratio on Exhaust Gas Temperature

It can be seen from this figure that HC emission is nearly constant at equivalence ratios lesser than 0.9 with percentage increase of 2.25% when equivalence ratio moved from 0.8 to 0.9. HC emission however increases sharply for equivalence ratios greater than 0.9 with percentage increase of 23.46% when equivalence ratio increases from 0.9 to 1.0. This figure also shows that HC emissions increase steadily with increase in engine speed at all equivalence ratios considered. The highest HC emission of 900ppm was obtained at engine speed of 4000rpm and equivalence ratio of 1.2 while the lowest emission of 466.7ppm was obtained at engine speed of 2000rpm and equivalence ratio of 0.8. This result may be due to the fact that better combustion is achieved at lower equivalence ratio of 0.8 provided that the mixture strength is not too lean and also that level of incomplete combustion increases with increase in equivalence ratios greater than 0.9. This trend is repeated for CO emission since both HC and CO emissions are products of incomplete combustion. Figure 12 shows that HC emission increases with increase in engine load with highest emission of 900ppm obtained at engine load of 100% and equivalence ratio of 1.2 while lowest emission of 400ppm was obtained at equivalence ratio of 0.8 and engine load of 0%. Figure 13 shows the effects of engine speed and equivalence ratio on CO emissions. It can be seen from the figure that, trend of CO emission is similar to that of HC emissions with lowest percentage increase of 0.96% when equivalence ratio increase from 0.8 to 0.9 and highest percentage increase of 37.14% when equivalence ratio increases from 0.9 to 1.0. The highest CO emission of 3200ppm was obtained at engine speed of 4000rpm and equivalence ratio of 1.2 while lowest CO emission of 1600ppm was obtained at engine speed of 2000rpm and equivalence ratio of 0.8. This result may be due to the fact that at lower speeds more time is available for better combustion.

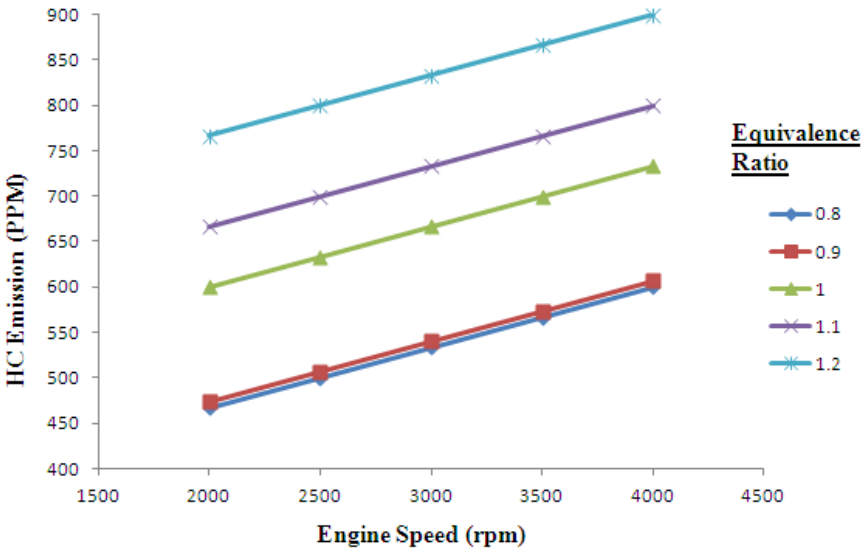

Figure 11: Effect of Engine Speed and Equivalence Ratio on HC Emission

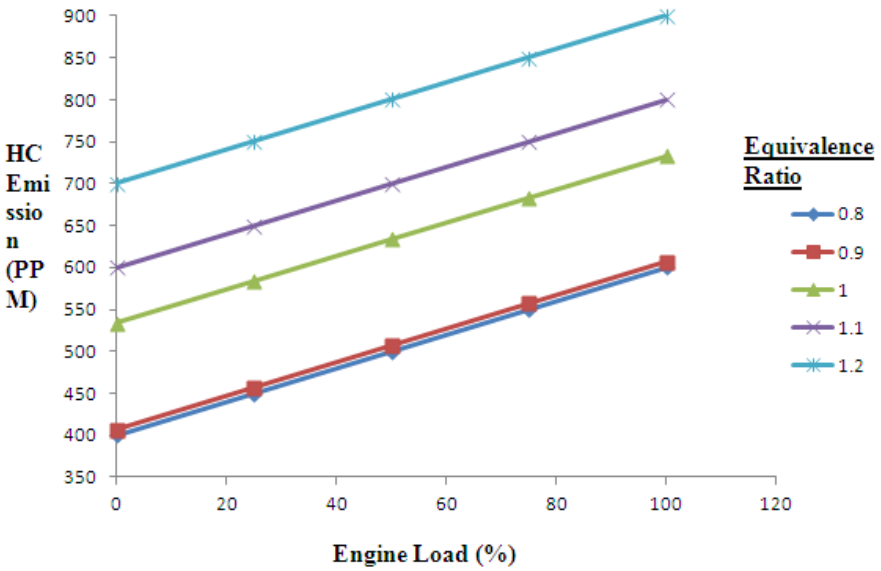

Figure 12: Effect of Engine Load and Equivalence Ratio on HC Emission

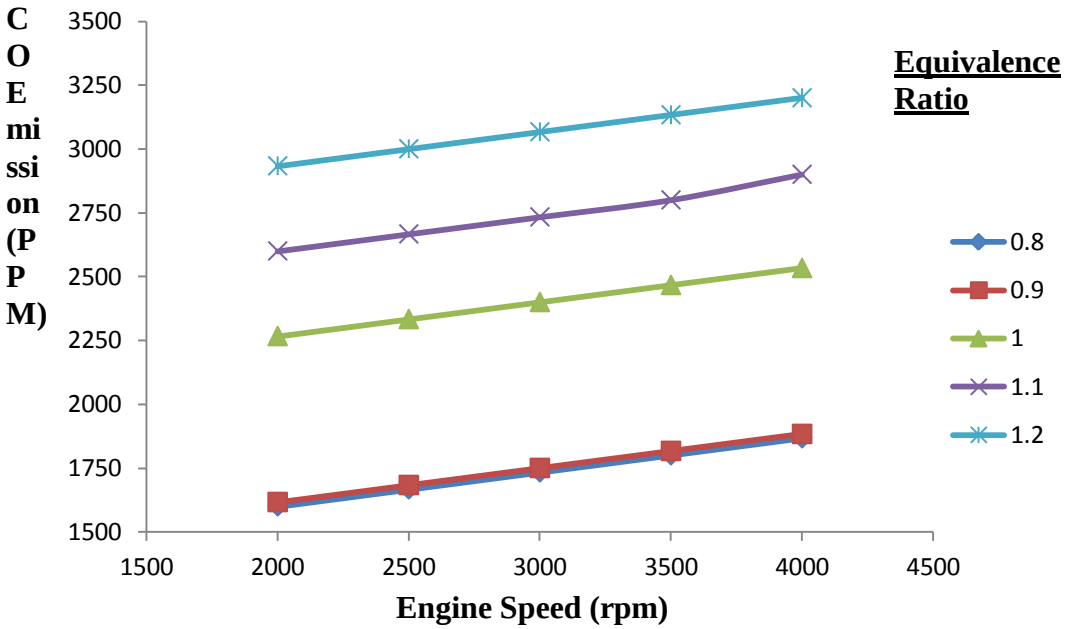

Figure 13: Effect of Engine Speed and Equivalence Ratio on CO Emission

Hence, CO and HC emissions tend to increase with increase in engine speed since they are products of incomplete combustion. Figure 14 shows that CO increased with increase in engine load and equivalence ratio. Highest CO emission of 3200ppm was obtained at engine load of 100% and equivalence ratio of 1.2 while lowest CO emission of 1533.3ppm was obtained at engine load of 0% and equivalence ratio of 0.8. Figure 15 shows the effects of engine speed and equivalence ratio on NO_x emission. It can be seen from the figure that engine speed of 3000rpm gives the highest value for NO_x emission and this value reduces before and after this speed. This figure also shows that NO_x emission increases sharply from equivalence ratio of 0.8 until this emission peaked at equivalence ratio of 0.9 before it reduces when equivalence ratio increases from 0.9 to 1.2. The highest NO_x emission of 326.7ppm was obtained at engine speed of 3000rpm and equivalence ratio of 0.9 while the lowest emission of 233.3ppm was obtained at engine speed of 2000rpm and equivalence ratio of 1.2. The result may be because NO_x formation is influenced by both higher cylinder temperature and higher oxygen (O_2) concentration in the cylinder. However as the equivalence ratio increased from 0.8, peak cylinder temperature increased moderately and cylinder O_2 concentration reduces drastically, hence NO_x emission tends

to peak around equivalence ratio of 0.9. Figure 16 shows the effects of engine load and equivalence ratio on NOx emission. It can be seen from the figure that NO_x emission peaked at equivalence ratio of 0.9 and engine load of 100%. The lowest NO_x emission of 176.7ppm was obtained at equivalence ratio of 1.2 and engine load of 0% while the highest emission of 310.0ppm was obtained at equivalence ratio of 0.9 and engine load of 100%.

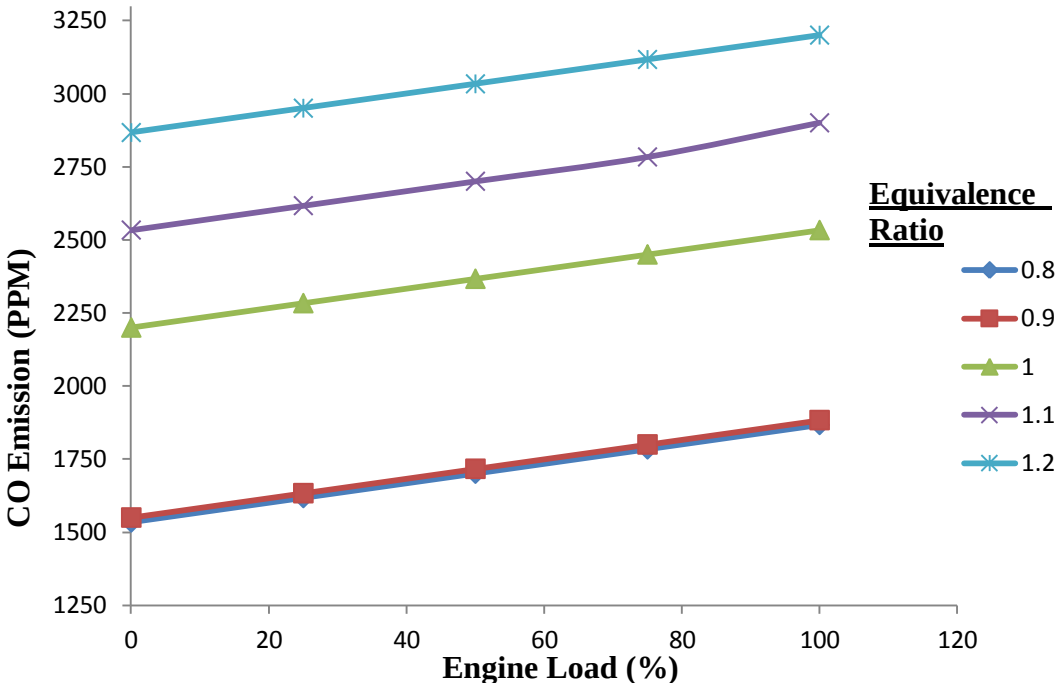

Figure 14: Effect of Engine Load and Equivalence Ratio on CO Emission

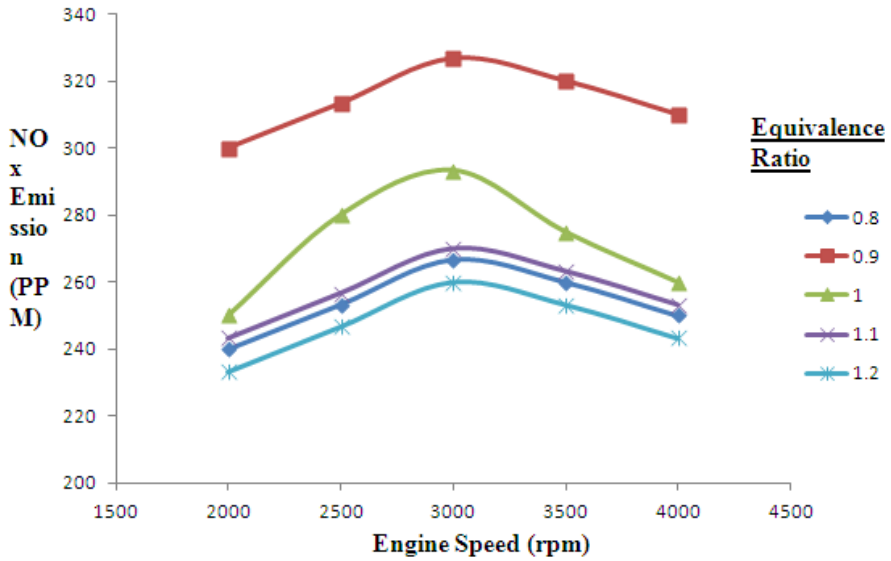

Figure 15: Effect of Engine Speed and Equivalence Ratio on NOx Emission

Statistical Evaluation

In this section ANN predicted results were compared with their corresponding results obtained from theoretical and experimental evaluations using t-test for two samples assuming unequal variances.

t-test for ANN and theoretical results

Table 3 shows the summary of t-test results obtained during comparison of ANN with theoretical results. From this table, it can be seen that for BMEP t stat value of 0.1083186 is less that t critical (two tail) value of 1.9627654 hence, the null hypothesis is accepted. For thermal efficiency, p(two tail) value of 0.9828987 is greater than the significance level of 0.05. This indicates that there is 98% chance that there is no significant difference between the two sets of results; hence the null hypothesis is accepted. HC emission has t stat value of -0.1375012 which is less than t critical (two tail) value of 1.9627654, hence the null hypothesis is accepted since t stat < t critical. For CO emission, p(two tail) value of 0.9855860 is greater than the significance level of 0.05. This shows that there is 98% chance that there is no significant difference between the two sets of results; hence the null hypothesis is accepted. For NO_x emission, t stat value of -0.3262459 is less than the t critical (two tail) value of 1.9640274 hence, the null hypothesis is accepted. It can be seen from this table that for all the five parameters p-value is much greater than 0.05 and t stat is less than t critical (two tail). Hence owing to these, the null hypothesis which states that there is no significant difference between the corresponding results is accepted for all the five parameters considered.

Table 3: Summary of t test for theoretical results against ANN predicted results

S/N	Parameter	t stat	t critical (two-tail)	P (two tail)	α	Comment
1.	BMEP	0.1083186	1.9627654	0.9137685	0.05	No Significant difference
2.	Thermal Efficiency	0.0214411	1.9627654	0.9828987	0.05	No Significant difference
3.	HC emission	-0.1375012	1.9627654	0.8906672	0.05	No Significant difference
4.	CO emission	-0.0180715	1.9627654	0.9855860	0.05	No Significant difference
5.	NO_x emission	-0.3262459	1.9627654	0.7443549	0.05	No Significant difference

t test for ANN and Experimental Results

Table 4.4 shows the summary of t test results obtained when ANN predicted results are compared with their corresponding experimental results. It can be seen from this table that for BSFC, t stat is -0.0084741 which is less than t critical (two tail) value of 1.9627654 and p (two tail) value of 0.9932406 is much greater than 0.05 significant level hence, the null hypothesis is accepted. For BP, p (two tail) value of 0.9382252 is greater than 0.05, this indicates that there is no significant difference between the two sets of results. EGT has t stat value of 0.1798377 which is less than t critical (two tail) value of 1.9627687 hence, the null hypothesis is accepted. Considering the table, it could be deduced that, at the overall the null hypothesis is accepted for all the three parameters considered.

Development of predictive models for the selected engine performance parameters using Design Expert Software

Response 1: BMEP

In order to describe the variation of this response, BMEP with independent variables and to test for its adequacy, the design programme suggested a quadratic model. The Model F-value of 1058.79 means the model is significant (Table 5). There is only a 0.01% chance that a "Model F-Value" this large could occur due to noise (Oladapo and Akanbi, 2015; Onawumi *et al.*, 2016). Values of "Prob > F" less than 0.0500 indicate model terms are significant. In this case A, B, C, B^2, C^2 are significant model terms. Values greater than 0.1000 indicate the model terms are not significant. If there are many insignificant model terms (not counting those required to support hierarchy), model reduction may improve the model. The "Pred R-Squared" of 0.9951 is in reasonable agreement with the "Adj R-Squared" of 0.9973 (Table 6). The ratio of 123.748 indicates an adequate signal. This model can be used to navigate the design space (Aremu *et al.*, 2014; Onawumi *et al., 2016*).

Table 4: Summary of t test for experimental results against ANN predicted results

S/N	Parameter	t stat	t critical two-tail	P (two tail)	α	Comment
1.	BSFC	-0.0084741	1.9627654	0.9932406	0.05	No Significant difference
2.	BP	0.0775236	1.9627654	0.9382252	0.05	No Significant difference
3.	EGT	0.1798377	1.9627687	0.8573229	0.05	No Significant difference

Table 5: ANOVA for response surface quadratic model (BMEP)

Source	Sum of Squares	DF	Mean Square	F-Value	Prob > F	
Model	1.106E+005	**9**	12289.60	1058.79	< 0.0001	Significant
A	*56101.33*	1	*56101.33*	*4833.33*	*< 0.0001*	
B	*143.37*	1	*143.37*	*12.35*	*0.0027*	
C	*36946.68*	1	*36946.68*	*3183.09*	*< 0.0001*	
A^2	*17.45*	1	*17.45*	*1.50*	*0.2368*	
B^2	*16051.13*	1	*16051.13*	*1382.86*	*< 0.0001*	
C^2	*1325.12*	1	*1325.12*	*114.16*	*< 0.0001*	
AB	*9.36*	1	*9.36*	*0.81*	*0.3816*	
AC	*6.90*	1	*6.90*	*0.59*	*0.4513*	
BC	*5.07*	1	*5.07*	*0.44*	*0.5175*	
Residual	197.32	17	11.61			
Cor Total	1.108E+005	27				

Table 6: Model estimation result

Response	BMEP	Thermal Efficiency	HC Emission	CO Emission	NOx Emission
R-Squared	0.9982	0.9953	1.0000	1.0000	0.9867
Adj- R-Squared	0.9973	0.9929	1.0000	1.0000	0.9796
Pred R-Squared	0.9951	0.9867	1.0000	1.0000	0.9692
Adeq Precision	123.748	78.751	1449.729	3499.902	42.610
Std. Dev.	3.41	0.61	0.72	1.44	4.66
Mean	219.91	34.17	579.14	2236.11	222.29
C.V.	1.55	1.79	0.12	0.064	2.10
PRESS	544.45	18.12	23.78	68.69	853.23

Other responses were further analysed following the same processes and the results are as presented in Tables 6 and 7.

Presentation of model equations for performance characteristics

All the model equations are given in terms of coded factors and the input parameters are as stated below for all the equations;

A = Load (%),

B = Speed (rpm),

C = Equivalent ratio and

E = Exponential function

Response 1: BMEP (kPa)

$$BMEP = +245.62 + 55.83*A + 2.82*B + 45.31*C - 1.71*A^2 - 51.72*B^2 + 14.86*C^2 + 0.88*A*B + 0.76*A*C - 0.65*B*C$$

Response 2: Thermal Efficiency (%)

The model equation is given as:

$$\text{Thermal Efficiency} = +40.26 - 2.82*A + 2.18*B - 6.36*C + 0.53*A^2 - 7.80*B^2 - 1.87*C^2 + 0.47*A*B + 0.58*A*C + 0.46*B*C$$

Response 3: HC Emission (ppm)

The model equation is given as:

$$\text{HC Emission} = +567.38 + 99.87*A + 66.84*B + 149.91*C + 0.13*A^2 + 0.38*B^2 + 17.13*C^2 - 0.26*A*B + 0.22*A*C + 8.333E\text{-}003*B*C$$

Response 4: CO Emission (ppm)

The model equation is given as:

$$\text{CO Emission} = +2236.11 + 167.21*A + 133.14*B + 667.44*C$$

Table 7:Design data for performance parameters

Study Methodology: Response Surface Experiments:27

Blocks: No Block

Initial Design : Historical Data

Design Model: Quadratic

Response	Name	Minimum	Maximum	Unit	Trans	Model
1	BMEP	101.6	357.0	kPa	None	Quadratic
2	Thermal Efficiency	19.5	48.5	%	None	Quadratic
3	HC Emission	268.0	901.0	ppm	None	Quadratic
4	CO Emission	1270.0	3207.0	ppm	None	Linear

5	NOx Emission	167.0	293.5	ppm	None	Quadratic

Response 5: NOx Emission (ppm)
The model equation is given as:

$$NOx\ Emission = +252.75 + 33.26*A + 4.24*B - 3.89*C + 1.02*A^2 - 27.81*B^2 - 18.89*C^2 - 0.075*A*B + 0.42*A*C - 1.01*B*C$$

V. CONCLUSION

This study investigated the effects of three operating parameters on eight performance parameters of SI engines using theoretical, experimental and ANN methods. The following conclusions can be drawn based on the various results obtained in this work;

i. Engine speed of 3000rpm gave the peak value for most of the SI engine parameters investigated in this study and these values decreased before and after this speed.
ii. EGT, HC and CO emissions increased with increase in engine speed with highest value obtained at maximum speed of 4000rpm.
iii. All of the SI engine parameters investigated in this work except thermal efficiency increased with increase in engine load with highest value obtained at maximum load of 100%.
iv. Most of the parameters investigated peaked at maximum equivalence ratio of 1.2. highest NO_x emission was obtained at equivalence ratio of 0.9 and this emission decreased before and after this value.

VI. RECOMMENDATIONS

The following recommendations are made for further studies;

i. Compression ignition, CI engines should be investigated using the same methods.
ii. The performance parameters investigated should be increased to include gas exchange processes, cooling system and lubricating system.
iii. The effect of heat transfer on thermal efficiency of SI engines should be investigated.

REFERENCES

[1]. Aremu M. O., Oke E. O., Arinkoola A. O. and Salam K. K. (2014) 'Development of Optimum Operating Parameters for Bioelectricity Generation from Sugar Wastewater Using Response Surface Methodology'' Journal of Scientific Research & Reports 3(15): 2098-2109, 2014; Article no. JSRR.2014.15.009
[2]. Ayeb M., Lichetenthäler D., Winsel T., Theuerkauf H. J., (1998) SI Engine Modeling Using Neural Network, SAE Paper n. 980790, - SP-1357 pp. 107-115.
[3]. Bang-Quan H., Jian-Xin W., Ji-Ming H., Xiao-Guang Y. and Jian-Hua X., (2002). A study on emission characteristics of an EFI engine with ethanol blended gasoline fuels. 941867. *Atmospheric Environment*, www.elsevier.com/locate/atmosenv p 949–957
[4]. Barhm-Ab-Mohamad (2013) A simulate model for analyzing the effect of engine Design parameters on the performance and emissions of Spark ignition engines
[5]. Baumann B. M., (1997) Intelligent Control Strategies for Hybrid Vehicles Using Neural Networks and Fuzzy Logic, Master Thesis, The Ohio State University,.
[6]. Charles, F. T., (2011) The Internal-combustion Engine. Books.google.co.in. 1985-01-01. ISBN 9780262700276. Retrieved 22/10/2011
[7]. Ciresan, D. C., Meier, U. Masci, J., Schmidhuber J., (2012) Multi-Column Deep Neural Network for Traffic Sign Classification. Neural Networks
[8]. De, J. N., Vianna, S., Do, A., Reis, V., De, A. B., Oliveira, S., Fraga, A. G. and De Sousa, M. T., (2005) Reduction of Pollutants Emissions on SI Engines - Accomplishments With Efficiency Increase. Journal of the Braz. Soc. of Mechanical Science & Engineering Vol. 27, No. 3: 217-222
[9]. Elijah I. and Asere A., (2008) A Comparative Performance and Exhaust Analysis of Blended Groundnut Oil and Mineral Oil Based Lubricant Using Spark Ignition Engine. Cigre Journal Manuscript EE07017volx.
[10]. Farley, B. G., and Clark W.A., (1954) "Simulation of Self-Organizing Systems by Digital Computer". *IRE Transactions on Information Theory* (4): 76–84. doi:10.1109/TIT.1954.1057468.
[11]. Frenklach, M., Packard, A., Seiler P. and Feeley R., (2004) Collaborative data processing in developing predictive models of complex reaction systems. International Journal of Chemical Kinetics, 36(1):57-66, doi: 10.1002/kin.10172.
[12]. Gosai D. C. and Nagarsheth H. J., (2014) Performance and Exhaust Emission Studies of an Adiabatic Engine with Optimum Cooling, 2nd International Conference on Innovations in Automation and Mechatronics Engineering, ICIAME.
[13]. Graves, A., Liwicki, M., Fernandez, S., Bertolami, R., Bunke, H. and Schmidhuber. J., (2009) A Novel Connectionist System for Improved Unconstrained Handwriting Recognition. IEEE Transactions on Pattern Analysis and Machine Intelligence, vol. 31, no. 5,
[14]. Hashemi S. H., Fard D., Almassi, M., Borghei, A. M. and Beheshti B. (2013) Simulation of Small Diesel Engine Vibration using Artificial Neural Network *International Journal of Agriculture and Crop Sciences.* IJACS/2013/5-18/2084-2090 ISSN 2227-670X ©2013 IJACS Journal Hecht-Nielsen R., (1987) *Neurocomputing*, Addison-Wesley.
[15]. Hinton, G. E., Osindero, S. and Teh, Y. W., (2006). "A Fast Learning Algorithm for Deep Belief Nets". *Neural Computation* 18 (7): 1527–554.:10.1162/neco.2006.18.7.1527. PMID 16764513. Edit
[16]. Holzmann H., Halfmann Ch., Isermann R., NeuroFuzzy (1998) Modeling of Automotive SI- Engine Characteristics, in proc. of IFAC Symposium Advances in Automotive Control 98, Mohican State Park, Loudonville, OH, USA, February 26 - March 1, pp.

156-160. *International Journal of Mechanical Engineering and Technology (IJMET)* volume 4, issue 5, September - October (2013) © iaeme issn 0976 – 6340 (print), ISSN 0976 – 6359
[17]. Jadhao, J. S. and Thombare, D. G., (2013) Review on Exhaust Gas Heat Recovery for I.C. Engine. International Journal of Engineering and Innovative Technology (IJEIT) Volume 2, Issue 12: 93-100. ISSN: 2277-3754; ISO 9001:2008 Certified
[18]. Jeffrey J. G. and Elliott N. G., (1993) Gasoline composition effects in a range of European vehicle technologies. SAE Technical Paper Series 932680.
[19]. Johan, W., (2003) "*Dynamics study of Automobile Exhaust System*."Department of Mechanical Engineering, Blekinge Institute of Technology, Sweden, Pg 1 - 45.
[20]. John M., (2012). "Scientists See Promise in Deep-Learning Programs". *NewYork Times*. November 23,
[21]. Keshav S. V. (2012) Control of Exhaust Emissions from Small Engines Using E-10 and E-85 Fuels Department of Mechanical Engineering University of Michigan- Dearborn Dearborn, Michigan 48128
[22]. Kraft M. and Mosbach S., (2009) The future of computational modelling in reaction engineering Technical Report 84, c4e-Preprint Series, Cambridge.
[23]. Lange, W. W., Muller, A., McArragher, J. S., and Schafer, V., (1994) The effect of gasoline composition on exhaust emissions from modern BMW vehicles. SAE Technical Paper Series
[24]. Manieniyan, V. and Sivaprakasam, S., (2013) Experimental Analysis of Exhaust Gas Recirculation on DI Diesel Engine Operating with Biodiesel. International Journal of Engineering and Technology Volume 3 No. 2: 129-135 ISSN: 2049-3444 © 2013 – IJET Publications UK.
[25]. McCulloch, W. and Walter P., (1943) "A Logical Calculus of Ideas Immanent in Nervous Activity". *Bulletin of Mathematical Biophysics* 5 (4): 115-133. doi:10.1007/BF02478259 McDonald, C. R., Shore, P. R., Lee, G. R., den Otten, J. and Humphries, D. T., (1994) The effect of gasoline composition on stoichiometry and exhaust emissions. SAE Technical Paper Series 941868.
[26]. Neimark, A., Kholmer, V. and Sher, E., (1994) The effect of oxygenates in motor fuel blends on the reduction of exhaust gas toxicity. SAE Technical Paper Series 940311.
[27]. Neural Information Processing Systems (NIPS) Foundation, (2009) pp. 545–552
[28]. Oladapo S. O. and Akanbi O. G. **(2015).** Models for predicting body dimensions needed for furniture design of junior secondary school one to two students. The International Journal of Engineering and Science (IJES) Volume 4 Issue 4 PP.23-36 ISSN (e): 2319 – 1813 ISSN (p): 2319 – 1805
[29]. Onawumi A. S, Adebiyi K. A., Fajobi M. O. and Oke, E. O. (2016) 'Development of Predictive Models for Some Anthropometric Dimensions of Nigerian Occupational Bus Operators' *European International Journal of Science and Technology ISSN: 2304-9693 www.eijst.org.uk*
[30]. Ortmann S., Glesner M., Rychetsky M., Tubetti P., Morra G., (2000) Engine Knock Estimation Using Neural Networks based on a Real-World Database, SAE Paper n. 980513, SP-1357, pp. 17-31. Patterson D. W., (1995) Artificial Neural Networks – Theroy and Applications, Prentice Hall,
[31]. Paykani A., Khoshbakhti R. and Shervani. M. T., (2011) "Experimental and numerical study of venturi EGR system in a dual fuel engine", *International Conference on Advanced Research and Applications in Mechanical Engineering*, Lebonan.
[32]. Rajput R. K., (2011) A Text Book of Automobile Engineering – R.K. Rajput – Google Books. Books.google.co.in. 2007-01-01. ISBN 9788170089919. Retrieved 2011-10-22.
[33]. Rajput, R. K., (2006) Thermal Engineering, Sixth edition, Laxmi Publications (P) LTD New Delhi, India. 1018-1171
[34]. Renhua F., Jing Y., Daming Z., Banglin D., Jianqin F., Jingping L. and Xiaoqiang L., (2013). Experimental study on SI engine fuelled with butanol–gasoline blend and H_2O addition *Energy Conversion and Management journal homepage:* www.elsevier.com/locate/enconman
[35]. Rochester, N., Holland, J. H., Habit, L. H. and Duda W. L., (1956) "Tests on a cell assembly theory of the action of the brain, using a large digital computer". *IRE Transactions on Information Theory* 2 (3): 80–93. doi:10.1109/TIT.1956.1056810. http://www.psych.utoronto.ca/users/reingold/courses/ai/cache/neural3.html
[36]. Ronald, D. M., (2006) Internal combustion engines. Mechanical Engineers' Handbook: Energy and Power, Volume 4, Third Edition. John Wiley & Sons, Inc.; Edited by Myer Kutz: 886-921.
[37]. Saravanan N. and Nagarajan G., (2008) "An experimental investigation on performance and emissions study with port injection using diesel as an ignition source for different EGR flow rates", *International Journal of Hydrogen Energy*, 33: 4456-4462,.(1)
[38]. Shivakumar, Srinivas P. P., ShrinivasaRao B. R. and Samaga B. S. (2010), performance and emission characteristics of a 4 stroke c.i. engine operated on honge methyl ester using artificial neural network ARPN Journal of Engineering and Applied Sciences Vol. 5, no. 6, June ISSN 1819-6608 ©2006-2010 Asian Research Publishing Network (ARPN).
[39]. Suvendu M. and Om Prakash, (2013) Analysis Of Exhaust Emission Of Internal Combustion Engine Using Biodiesel Blend *International Journal of Emerging Technology and Advanced Engineering* Website: www.ijetae.com (ISSN 2250-2459, ISO 9001:2008 Certified Journal, Volume 3, Issue 5, May)
[40]. Venkatasubramanian V., (2009) Drowning in data: Informatics and modeling challenges in a data rich networked world. AIChE Journal, 55(1):2-8, 2009. doi: 10.1002/aic. 11756.
[41]. Wallington, T. J., Kaiser, E. W. and Farrell, J. T. (2006) Automotive Fuels and Internal Combustion Engines: A Chemical Perspective. Chemical Society Review, 35:335–347. www.rsc.org/csr

ADIO, T. A, et. al. "Evaluation of Performance Parameters of Spark Ignition Engine Using Artificial Neural Network."*American Journal of Engineering Research (AJER)*, vol. 10(4), 2021, pp. 15-35.